ISBN: 978-3-95450-262-2 ISSN: 2673-5350 doi: 10.18429/JACoW-IBIC2025-WEBC02

LESSONS LEARNED IN COMMISSIONING THE NEW BEAM-LOSS MONITORS FOR THE SUPERCONDUCTING UPGRADE TO LCLS*

A. S. Fisher†, G. W. Brown, E. P. Chin, S. Chowdhury, W. G. Cobau, J. E. Dusatko, B. T. Jacobson, T. Kabana, K. Kruchinin, R. S. M. Martinez, J. Pigula, Evan Rodriguez
SLAC National Accelerator Laboratory, Menlo Park, California, USA

Abstract

The superconducting upgrade to the LCLS x-ray free-electron laser at SLAC is now in commissioning, as we gradually raise the repetition rate of the 4 GeV beam toward 1 MHz and the beam power toward 120 kW. A further upgrade in 2026 will double the energy and power. Machine protection at this extremely high power required a novel system of fast beam-loss monitors (BLMs). Points of concern, such as collimators or kickers, are covered by diamond detectors (PBLMs). Long optical fibres (LBLMs) of up to 200 m span the entire 4 km facility, generating and capturing Cherenkov emission from beam-loss showers. Previous papers have reported on the design and early commissioning of this safety system, and on plans to use the loss signals for wire scanners and loss localisation. Subsequent experience in commissioning and operating the full system has demonstrated that the concept is sound and sensitive, but several aspects of the implementation have proven troublesome. Extensive testing and debugging uncovered issues with both hardware and firmware. We will detail these problems, their remedies, and the improvements in performance.

INTRODUCTION

Over the past decade, SLAC installed and has been commissioning the new 700 m superconducting (SC) linac that replaced the first 1 km of its original 3 km normal-conducting (NC) copper linac. Using continuous-wave 1.3 GHz radio-frequency (RF) power, the new 4 GeV accelerator is gradually being ramped up to a beam power of 120 kW with a pulse rate of up to 929 kHz. In 2026, the High-Energy (HE) upgrade will install additional cryomodules to double the beam's energy and power. With a high risk of damage from this beam power, we replaced our previous beam-loss monitors (BLMs) based on ionization chambers, which are limited by the slow transport of ions [1], with new, faster BLMs. Expected loss points are now protected by point BLMs (PBLMs) using 4-mm-square diamond detectors from Cividec (type B1-HV). The entire 4 km beam path is monitored by long BLMs (LBLMs) using radiation-hard optical fibres from the Polymicro division of Molex (FBP600660710). The new BLMs and the signal processing were described in [2-7].

Initial commissioning [4, 5] showed good sensitivity and fast response, with the linac still at low rate. Further experience at higher loss power uncovered several performance problems, especially with the LBLMs—not with the fibres themselves but with the associated photomultiplier tubes (PMTs), electronics, and processor software. Some issues are common to the PBLMs. This paper presents these problems and their resolutions, to update those who might want to replicate our approach.

* SLAC is supported by the U.S. Department of Energy, Office of Science, under contract DE-AC02-76SF00515.
† afisher@slac.stanford.edu

LONG BEAM-LOSS MONITORS

Layout

When a beam-loss shower passes through the optical fibre of an LBLM, some of the emitted Cherenkov radiation is captured in the fibre and carried to the ends. The fibres are typically 200 m long, but shorter lengths span specific segments of the machine, such as the L2 section of the SC linac (between bunch compressors 1 and 2) or a warm section for compression, collimation, or diagnostics. Each fibre runs between two chassis in electronics racks outside the tunnel. In each chassis, which is both the end of one fibre and the start of the next, a PMT measures light arriving at one fibre's downstream end, and a modulated LED sends weak light into the upstream end of the next, as a continuous self-check. A motherboard both processes the PMT signal and drives the LED.

After outlining the signal processing [6], we examine the problems with the PMTs, the self-check, and the electronics, as well as control of the PMT and LED temperatures.

Integrated Loss Signal

A passive filter (Fig. 1) splits the PMT signal into low and high frequencies, V_L and V_H. For V_L, charge from the PMT accumulates immediately on capacitor C_1 and discharges through R_1 with a time constant R_1C_1 = 500 ms. This integrated signal measures the beam's loss rate independently of its repetition rate.

A buffer op amp multiplies V_L by a gain G ($1 \le G \le 74$) that matches the sensitivity needed for each fibre. In the warm regions separating linac sections, $G = 6$. In cold sections, where losses must pass through the thick steel of the cryostat housing, $G = 50$. Along the 2 km bypass beamline over the NC linac, where the fibre is only 40 cm above the SC beam, $G = 1$. Most other locations use $G = 20$.

An analogue comparator stops the beam if GV_L exceeds the threshold selected for the Beam Containment System (BCS). The same GV_L is buffered and sent outside the chassis to a node of the Machine Protection System (MPS) in an ATCA crate, where it is digitised and compared to a separate threshold [2]. Depending on the location, the MPS can block the photocathode laser, lower the beam rate, or stop a kicker from sending beam into a specific beamline. The BCS shuts off RF power to the electron gun. Because recovery is slow from a BCS trip, the MPS threshold is set

ISBN: 978-3-95450-262-2 ISSN: 2673-5350 doi: 10.18429/JACoW-IBIC2025-WEBC02

below that of BCS. In most cases only the MPS should trip. The two systems are designed to bring the loss signal below threshold within 100 μs.

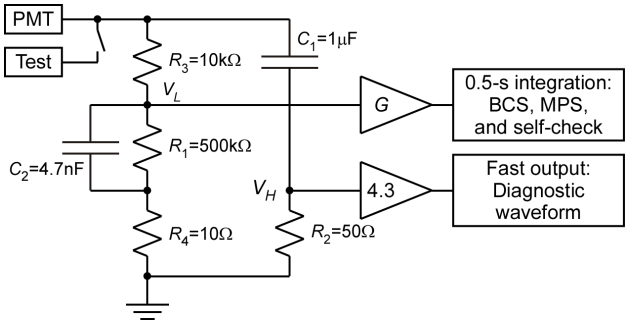

Figure 1: PMT pulses immediately charge C_1 to produce the integrated signal V_L, which decays with time constant R_1C_1 = 500 ms. Typical values of R_1 and C_1 are shown, but they vary with location, as does the buffer amplifier's gain G. Capacitor C_2, across R_1, removes fast PMT spikes from V_L. High frequencies, terminated by R_2, produce the waveform V_H, used for diagnostics such as loss localisation.

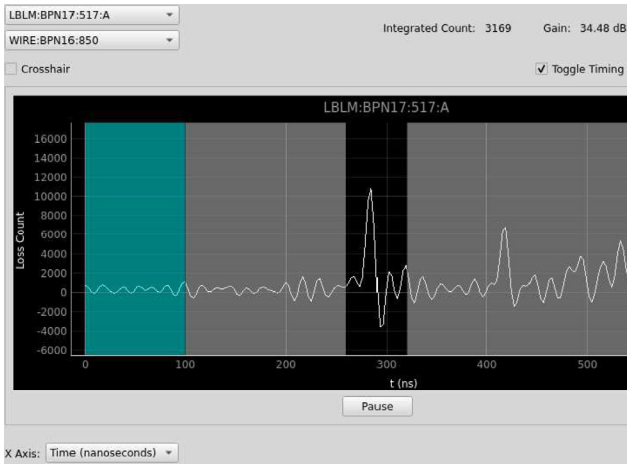

Figure 2: Fast loss waveform showing a peak from a wire scanner vs. time (ns). The peak in the black region at centre is loss from the wire. This is integrated numerically for plotting against wire position, after subtracting the pedestal measurement from the green region at left.

Fast Loss Waveform

The high-frequency signal V_H supports loss diagnostics. After its buffer op amp, V_H goes to an external amplifier with an adjustable gain from −27 to +57 dB next to an ATCA crate, where the waveform is digitised.

Loss locations are determined by the arrival time t of the waveform's leading edge. To calibrate the longitudinal coordinate z against t, the beam strikes a known loss point such as a screen or collimator jaw. The speed of light in the fibre then identifies loss positions along the fibre.

Additional peak(s) appear on the waveform when a wire scanner passes a set of wires through the beam (Fig. 2). The waveform from each bunch is integrated numerically across the peak(s) and plotted against wire position to obtain a beam profile. However, since a thin wire scatters only a small portion of the bunch charge, the signal can be low. Moreover, the small scattering angle spreads losses along some 50 to 100 m of fibre downstream of the wire (unless a bend increases the angle of the degraded electrons). The gain of the op amp buffering V_H was recently raised from 1 to 4.3. Gain before the long cable to the variable-gain amplifier can improve the signal-to-noise ratio.

Photomultipliers

PMTs in the LBLMs have red-sensitive photocathodes, because attenuation in both new and irradiated fibres is strong for blue light but minimal for red and near-infrared [7]. However, elevated dark current due to the low work function of such cathodes must be countered by cooling. We chose Hamamatsu's H7422P-40 PMT module, which includes both an internal Peltier (thermoelectric) cooler to hold the photocathode at 0 °C and also a DC-to-DC converter generating the high voltage for the PMT bias from the +12 V supply and a low-voltage control input.

After about two years of operation, most PMTs rapidly lost response or failed entirely. Hamamatsu replied that the GaAsP photocathode is "sensitive" and subsequently provided a plot, extrapolated from their tests, predicting that the anode current (~1 nA) from our very small self-check could cause a gradual output drop of ~30 % after 20,000 hours (2.3 years) of operation. This hints at the cause but without accounting for the total failure of many PMTs.

Hamamatsu replaced our model with its H16722P-40. The old and new types share the same housing, control cable, and control board. However, the newer one is said to be more "robust", with the specification for the time-averaged "maximum output signal current" raised from 2 to 40 μA. The maximum gain is also doubled. Following Hamamatsu's advice, we now use this newer type.

Self-Check

Our weekly testing to verify BCS functionality will be wholly inadequate as the beam power rises toward the goal of 250 kW. Instead, the self-check constantly monitors the complete signal path of each BLM. If, for example, a PMT bias supply suddenly fails, the resulting self-check fault will trip BCS within minutes, as the filtered signal decays.

In the self-check, a sinusoidally modulated LED sends weak light into the fibre's upstream end. At the other end, the PMT detects this light along with light captured in the fibre from beam loss. On the motherboard, an analogue filter followed by digital filters in the processor—acting like a digital lock-in amplifier—recover the self-check amplitude despite the presence of a larger loss signal and despite the lowest possible LED illumination.

The modulation frequency must be low for transmission through the 500 ms filter for V_L. Initially, the LED current had a period of 1.25 s (0.80 Hz). To avoid any low-order resonance between the modulation and our lowest beam rates, 1 and 10 Hz, the period was changed to 1.30 s (f_m = $\omega_m/(2\pi)$ = 0.769 Hz).

Our "Archiver" records the detected self-check amplitude every second. Over the long-term, we obtain a continuous record of PMT and fibre health, indicated by a slow degradation of the amplitude despite a constant LED drive.

ISBN: 978-3-95450-262-2 ISSN: 2673-5350 doi: 10.18429/JACoW-IBIC2025-WEBC02

Periodic tests with a calibration lamp can determine whether the decline is from a slow drop in PMT response or greater radiation-induced fibre attenuation. First, the lamp is connected to the PMT through a short test fibre. We note the control voltage (the input to the DC-to-HV converter) needed to generate 1 μA into a picoammeter. Next, light from the lamp is passed through the fibre to the PMT and the motherboard electronics. We compare the control voltage needed to produce 500 mV at the MPS output of the chassis with both this long fibre and with the short fibre. After accounting for the exponential rise in gain with voltage, we obtain the fibre attenuation.

The PMT failures led us to further reduce the light level used for the self-check. We first changed to low-current LEDs. For stability, the LED drive circuit regulates the current, not the voltage; however, emission from an LED still requires some minimal current for a reasonably linear and stable turn on. To make the LED brighter while coupling less of the light into the fibre, we inserted a 10 dB black optical filter between the LED and the fibre tip and spaced the tip an additional 8 mm from the LED.

PMT and LED Temperatures

Hamamatsu warns that the internal cooler of the PMT cannot maintain a temperature difference greater than 35 °C between the photocathode and the PMT housing (but other Hamamatsu documentation suggests 25 °C). LBLM electronics are largely placed in enclosed, fan-cooled racks in support buildings above the accelerator tunnel. These buildings, like the 3 km Klystron Gallery, are mostly simple sheds without heating or cooling, due to the mild California climate. However, through the year the ambient temperature inside racks can range from 10 to 45 °C. To keep the PMT housing below 35 °C, the rear panel of the chassis included a secondary Peltier cooler (TE Technology CP-040HT). Above 30 °C, this removed heat from the housing via thick aluminium blocks.

We chose an LED as the self-check source without considering that LED emission drops with temperature [5]. Wide temperature swings from a cold night to a hot afternoon led to a diurnal change in the detected self-check—sometimes with large jumps as the Peltier switched on and off (Fig. 3a)—that could cause a BCS fault at either extreme. The additional seasonal change made it impossible to set a stable self-check level for long-term monitoring.

We initially attempted to reduce the change by inserting a series resistor with a negative temperature coefficient into the LED current control, lowering the current when cold and raising it when hot [5]. After this simple open-loop approach proved inadequate, we redesigned the temperature control inside the chassis.

In a Peltier device, current across a semiconductor junction transfers heat from one side to the other. The sides switch roles by simply reversing the current polarity. We replaced the original control board, which offered only cooling, with one that is bipolar and supports precise PID (proportional, integral, derivative) regulation (TE Technology TC-36-25-RS232). Additional aluminium blocks extend the thermal path to the LED and fibre tip. The feedback thermistor was moved from the PMT housing to the LED block. The LED remains within ±0.1 °C (Fig. 3b) of the new 24 °C setpoint. The PMT, between the Peltier and LED, stays at 24 ± 2 °C, with the sign following the direction of heat flow from the Peltier. The PMT module's internal Peltier cooler then holds the photocathode at 0 °C.

Processor Software

After the integrating filter and op amp, the signal GV_L splits to drive both BCS and MPS. A third path, for the self-check, passes through an analogue bandpass prefilter peaking at 0.56 Hz and dropping by 20 dB at 0.015 and 13 Hz. Its differential output goes to the analogue-to-digital converter (ADC) at the input of a processor (Texas Instruments TMS320F28377S) that implements sequential digital filters for more complete isolation of the self-check from the beam-loss signal.

The processor first shifts the modulation to baseband (DC) with an I&Q (in-phase and quadrature) digital mixer that multiplies the signal by $\cos(\omega_m t)$ and $\sin(\omega_m t)$. Originally, three cascaded digital low-pass filters followed: a 29-tap finite impulse response (FIR), a smoothed moving median (SMM), and a single-pole infinite impulse response (IIR) with a time constant $\tau_{IIR} = 51.2$ s. However, this filtering was found to be inadequate in the presence of low-rate beam losses, which made the detected self-check noisy and sensitive to temperature (Fig. 3a).

We pursued various improvements, beginning with simpler ones. The ADC sampling rate was raised from 10 Hz, which provided only 13 samples per period, to 1280 Hz. To equalise the expected self-check amplitude at every chassis, despite the wide range of op-amp gains G, the ADC output is multiplied by $69 / G$.

Next, a MATLAB model of the complete system—analogue and digital, including random beam loss and the modulation—compared various filter options. Two cascaded IIR filters, with $\tau_{IIR} = 204.8$ and 409.6 s, were promising. They performed mostly as expected until the linac rate was gradually raised to 16.6 and 33.2 kHz. Although the amplitude of the LED modulation at f_m remained constant, steady high-rate losses (common near collimators) often drove the detected self-check strongly toward zero (Fig. 3b). This was surprising: the spectrum of a single loss peak or low-rate random losses is broad enough to include a component at f_m. However, high-rate losses are smoothed by the 500 ms integrating filter, making them nearly constant with a minimal contribution at f_m. Our observations could not be reproduced with adjustments to the model by, for example, assuming correlations between losses over times <1 s.

We suspected a hardware problem, such as saturation of the analogue electronics. By slowly raising the modulation amplitude, we found that the self-check detected by the processor first increased but then decreased to nearly zero, although a spectrum analyser showed a large and clearly rising peak at f_m. We found no evidence of saturation or of reaching the input limits of the ADC.

ISBN: 978-3-95450-262-2 ISSN: 2673-5350 doi: 10.18429/JACoW-IBIC2025-WEBC02

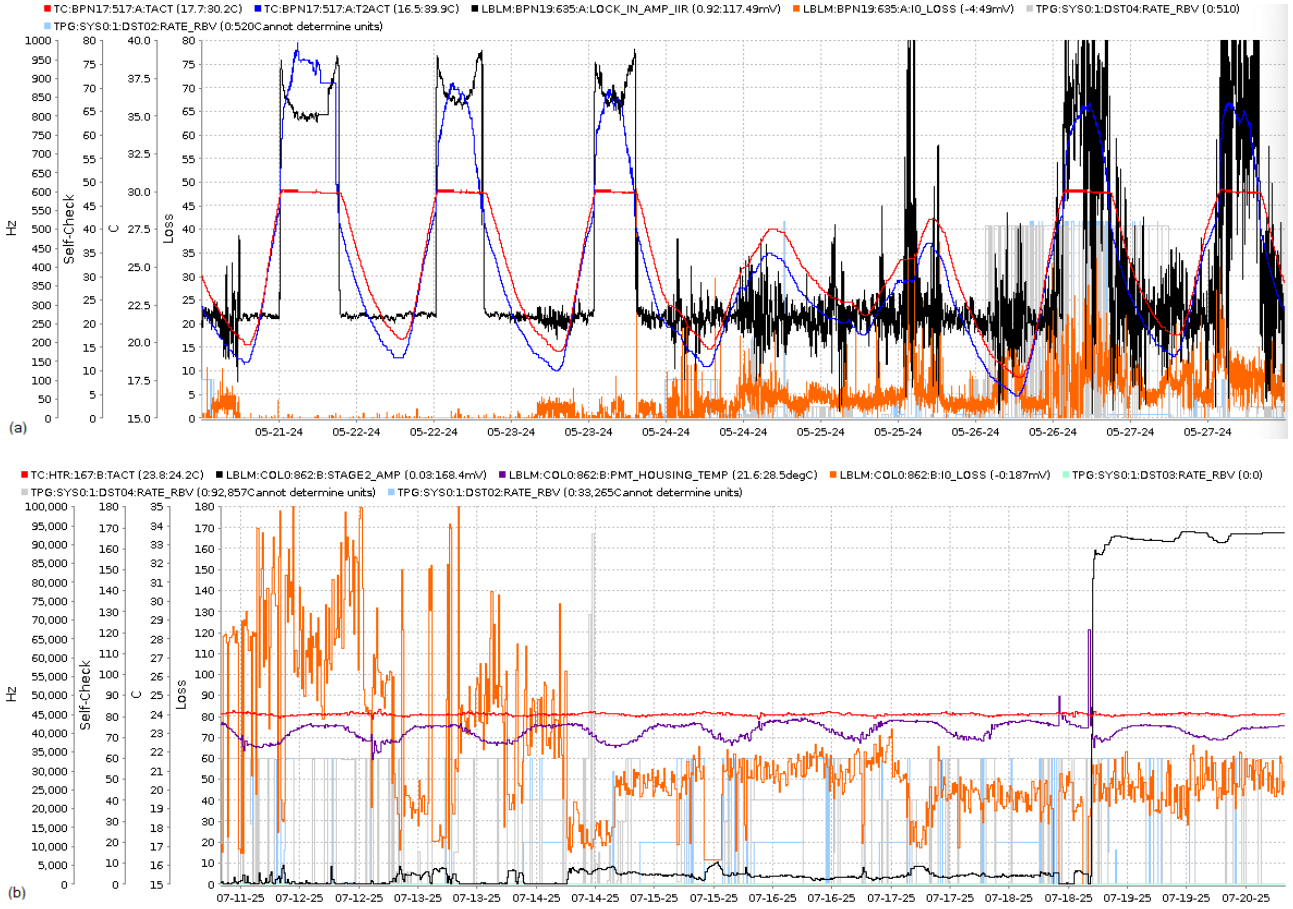

Figure 3: (a) Over 7 days, the original thermal control kept the PMT housing temperature (red) to a maximum of 30 °C even as the external (hot) side of the Peltier (blue) went to 40 °C. The self-check (black) jumped up/down when the Peltier switched on/off. Between the jumps, the self-check dipped as the temperature peaked. With these original filters, the self-check was strongly affected by beam loss (orange), with a beam rate (grey or light blue, depending on beamline) ≤500 Hz. (b) Over 9 days, the new thermal control keeps the LED at 24 °C (red). The PMT housing (violet) is ~1 °C colder as heat flows from the LED past the PMT to the Peltier, here in its cooling mode. At a 33 kHz beam rate (grey or light blue), losses (orange) strongly affect the self-check (black) despite newer filters (dual IIRs), at times driving it nearly to zero. After correcting the C code for the processor (right, July 18), the self-check level became both larger and more stable.

The ADC and the software were carefully re-examined with a processor on a test board. We found problems stemming from the peculiar version of C used by the compiler for the processor. Our calculations require double precision, but the compiler applies single precision unless variables are declared not as “double” but as “long double”. Moreover, double-precision constants are interpreted as single unless the letter “L” is appended after the last digit—for example, “6.0L”. These rules are not documented.

Three days before our 2025 summer maintenance shutdown, we tested two LBLMs with partly corrected code for the two IIR filters. The changes resulted in a detected self-check that was large and stable over two days (Fig. 3b).

We then tried a further improvement, replacing the first single-pole IIR with a 4th-order Chebyshev Type-1 filter with a bandwidth of 0.04 f_m. The second filter can be the single-pole IIR with τ_{IIR} = 204.8 s. These filters were first tested in MATLAB with LBLM beam-loss data recorded by an oscilloscope in three 17-minute intervals at three levels of modulation drive. However, our rushed test with beam in the final hours failed because the filter was unstable. We learned later that the double-precision constants needed as filter coefficients were treated as single.

Electronics on the Motherboard

Several major and minor design issues with the complex motherboard were found only after many boards were in use over an extended time. Corrections have been incorporated in a new version.

The large, fast loss peaks from the PMT were the most significant concern. Where these enter the input filtering circuit (Fig. 1), an analogue switch allows the introduction of a test pulse to check the full fault-detection chain. The loss peaks can reach as high as 30 V, exceeding the tolerance of the switch. Over time the switches in several LBLMs failed. We replaced the switch with a more robust type and added protection diodes.

More recently we realized that fast loss peaks also reach the op amp that buffers V_L and amplifies by G. So far, none have been damaged, but the spikes may exceed the slew

ISBN: 978-3-95450-262-2 ISSN: 2673-5350 doi: 10.18429/JACoW-IBIC2025-WEBC02

rate of the amp and cause nonlinearity. We added capacitor C_2 and a small resistor R_4 to the input filter (Fig. 1) to shunt high-frequency components to ground, slightly slowing the rise of V_L, without affecting the decay time constant.

The processor at the fibre's upstream end synthesizes the sine wave driving the LED modulation. The processor at the downstream end demodulates in a mixer with a cosine and sine at the same frequency. The separate 10 MHz crystal oscillators that clock these two frequency sources must not shift phase significantly over several filtering time constants. Our new oscillators are stable to 1 part per million.

For more stability in the LED current control, a fixed resistor replaced a potentiometer. The processor's DAC (digital-to-analogue converter) offers sufficient tuning range.

POINT BEAM-LOSS MONITORS

Instead of a chassis, the PBLM is housed in a double-width Small Instrumentation Module from Stanford Research Systems. The PBLM motherboard shares most of the LBLM circuitry and processor software, but in the module's smaller form factor. The integrating filter has a smaller C_1, to get more voltage from a smaller loss charge, and a larger R_1, to maintain the 500 ms time constant. A DC-to-DC converter inside the module provides the 250 V bias for the diamond chip. For a self-check, the bias is modulated by typically ±2.5 V at the same frequency used in the LBLMs, driving a small AC current through the diamond's 3 pF capacitance and into the signal-processing chain. There is no need for an LED or PMT, nor for thermal management. Because the same processor chip both modulates and demodulates, phase drift is not a concern.

Compared to LBLMs, most PBLMs used for BCS are unlikely to see large continuing beam losses, due to their locations and to the small signals from these devices. However, in certain instances the self-check has been impacted by losses. Lower loss spikes also mean that none of the analogue switches used for the test pulse has been damaged. We plan to upgrade the PBLM boards with the improvements found for the LBLMs. PBLMs still use the original processor code, with the original filters and the bug in the ADC setup. Once we have a final version of LBLM code, the new code will be implemented in the PBLMs.

CONCLUSION

Bringing an entirely new BLM system into full operation led to unanticipated difficulties and delays. Considerations of fibre attenuation required a cooled, red-sensitive PMT. The self-check illumination on the sensitive photocathode in Hamamatsu's earlier model led to shortened lifespans of about two years. These PMTs have been replaced with a newer type, but we have also adopted the philosophy that even these newer PMTs, although said to be more robust, must be tested at least annually. We now consider them to be consumables, to be replaced as needed but probably every few years. This approach contrasts with the far longer lifetimes of standard PMTs.

Weekly BCS tests will be replaced by a constant self-check of the functionality of the loss-monitoring system, essential for the 250 kW beam expected in 2027. The self-check can halt the beam in minutes and provides a method for tracking slow degradation of the PMT and fibre.

Commissioning brought other surprises, centred on the electronics and the software for the motherboard processor. Accumulated small hardware issues led to the need for a new version of the motherboard. Several revisions of the processor code have changed the digital filters and, most recently, fixed a major problem in the setup of the ADCs.

We have encountered several surprises in bringing an entirely new BLM system into full operation. Nevertheless, the fundamental concept remains sound, and persistent investigation has led us to solutions.

REFERENCES

[1] A. S. Fisher, R. C. Field, and L. Y. Nicolas, "Evaluating Beam-Loss Detectors for LCLS-2", in *Proc. IBIC'16*, Barcelona, Spain, Sep. 2016, pp. 678-681. doi:10.18429/JACoW-IBIC2016-WEPG23

[2] A. S. Fisher *et al.*, "Beam Containment and Machine Protection for LCLS-2", in *Proc. IBIC'17*, Grand Rapids, MI, USA, Aug. 2017, pp. 478-481. doi:10.18429/JACoW-IBIC2017-TH1AB2

[3] A. S. Fisher *et al.*, "Beam-Loss Detection for LCLS-II", in *Proc. IBIC'19*, Malmö, Sweden, Sep. 2019, pp. 229-232. doi:10.18429/JACoW-IBIC2019-TUAO02

[4] A. S. Fisher *et al.*, "Commissioning Beam-Loss Monitors for the Superconducting Upgrade to LCLS", in *Proc. IBIC'22*, Kraków, Poland, Sep. 2022, pp. 207-210. doi:10.18429/JACoW-IBIC2022-TU2C3

[5] A. S. Fisher *et al.*, "Commissioining the beam-loss monitoring system of the LCLS superconducting linac", in *Proc. IBIC'23*, Saskatoon, SK, Canada, Sep. 2023, pp.187-190. doi:10.18429/JACoW-IBIC2023-TUP005

[6] J. E. Dusatko, A. S. Fisher, E. P. Chin, Evan Rodriguez, G. W. Brown, and W. G. Cobau, "The LCLS-II beam loss monitor readout system", in *Proc. IPAC'24*, Nashville, TN, USA, May 2024, pp. 3362-3365. doi:10.18429/JACoW-IPAC2024-THPG44

[7] A. S. Fisher, *et al.*, "Beam-loss detection for the high-rate superconducting upgrade to the SLAC Linac Coherent Light Source", *Phys. Rev. Accel. Beams*, vol. 23, p. 082802, 2020. doi:10.1103/PhysRevAccelBeams.23.082802